Characteristics of an atmospheric microwave-induced plasma generated in ambient air by an argon discharge excited in an open-ended dielectric discharge tube

Se Youn Moon and W. Choe[a)]
Department of Physics, Korea Advanced Institute of Science and Technology, 373-1 Kusong-dong, Yusong-gu, Taejon 305-701, Korea

Han S. Uhm
Ajou University, San 5 Wonchon-dong, Paldal-gu, Suwon 442-749, Korea

Y. S. Hwang
Seoul National University, San 56-1 Shilim-dong, Kwanak-gu, Seoul 151-742, Korea

J. J. Choi
Kwangwoon University, 447-1 Wallkye-dong, Nowon-gu, Seoul 139-701, Korea

(Received 19 February 2002; accepted 29 May 2002)

Parametric observations on an atmospheric-pressure plasma sustained in ambient air by an argon discharge excited by 2.45 GHz microwaves in an open-ended dielectric discharge tube are reported. Microwave power, discharge tube dimensions, and argon flow rate were the major operating parameters. Three distinctive plasma regions were observed: plasma filaments exiting from the discharge tube, converging point of these filaments, and a plasma flame. At the filament-converging point, argon atom excitation temperature, rotational temperature, and electron density were measured by optical emission spectroscopy (OES) in the operating range of (3.0–5.0) liters per minute of gas flow rate and (650–950) W of microwave power. The measured excitation temperature and rotational temperature were (5000–5800) K and (2800–3400) K, respectively. The electron density obtained by Stark broadening width of the H_β line showed $(5.0-8.0)\times 10^{14}$ cm^{-3}. It was observed that the volume of the plasma flame and the gas temperature were increased with increasing the microwave power. On the other hand, higher gas flow rates increased the electron density. In the plasma flame, the gas temperature measured by a thermocouple and OES was in the range of (1030–2200) K, which showed an exponential decrease in the axial direction away from the converging point. © *2002 American Institute of Physics.*
[DOI: 10.1063/1.1495872]

I. INTRODUCTION

Atmospheric microwave induced plasma (MIP) sources have been studied for decades due to their many advantages, such as the lack of the necessity for expensive vacuum equipment, low cost and simple systems, and easy operation. Because of these advantages, many types of atmospheric MIP sources have been developed. In particular, the MCFR (Microwave Continuous Flow Reactor),[1,2] SWSP (Surface Wave Sustained Plasma),[3] TIA (Torch with Axial gas Injection),[4,5] MPT (Microwave Plasma Torch),[6] and Microwave Cavity plasma[7,8] are well-known types of plasma sources using microwaves. The main application areas for these plasma sources have been in real-time metal emission monitoring,[2,9] surface treatment, remediation of gases, and atomic spectrometry.

For diagnostics, the electrostatic Langmuir probe method that is widely used for low pressure plasmas is generally less useful for plasma produced at atmospheric pressure. This is because the electron-neutral collision mean free path is much smaller than the probe dimension, so the usual collisionless-sheath model is not applicable. In the case of air, for example, the electron–air molecule collision cross section is 1.3×10^{-15} cm^2. When electron energy is 1 eV, the electron–air molecule collision frequency is of the order of 10^{10} s^{-1}, and the mean free path is only about 0.3 μm.[10,11] Therefore, other diagnostic methods are needed to measure plasma parameters, and optical emission spectroscopy (OES) has been used as one of the alternative diagnostics because of its simplicity and nonintrusive nature.

This work concerns an atmospheric microwave-induced plasma generated in ambient air by an argon discharge sustained in an open-ended fused silica discharge tube. This system of a simple design is adequate for studying the characteristics of atmospheric pressure plasma. Three distinctive regions were observed: plasma filaments exiting from the discharge tube, the converging point of these filaments, and a plasma flame. At the filament-converging point where the emission intensity was the largest, the argon atom excitation temperature and the rotational temperature of OH molecule were measured by OES. The electron density was obtained from the Stark-broadening width of the H_β emission line

[a)]Author to whom correspondence should be addressed. Electronic mail: wchoe@mail.kaist.ac.kr

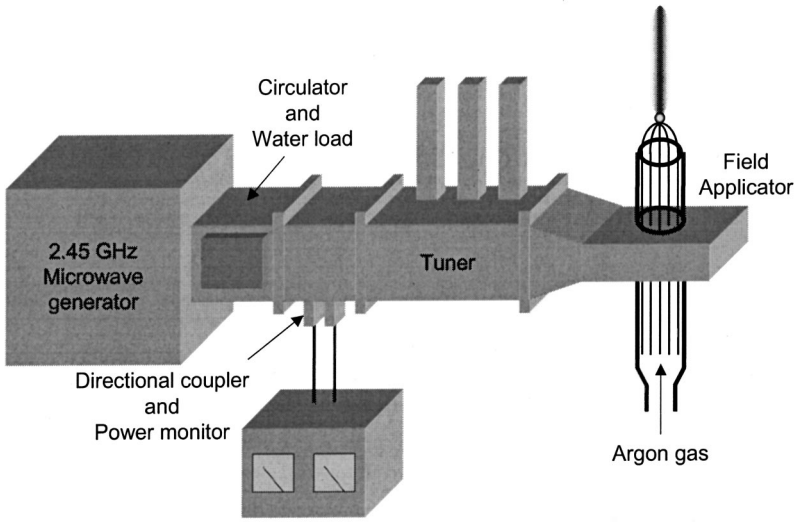

FIG. 1. Experimental setup of the atmospheric microwave-induced plasma. A fused silica tube of 18 mm inner diameter in which plasma is generated is inserted perpendicularly to the wide wall of the WR-284, wave guide. Argon gas is introduced from underneath the tube to provide the plasma source. The top of the tube is open to the air.

profile. The gas temperature was measured at the plasma flame with a thermocouple. Based on the measurements at different microwave power levels and gas flow rates, investigation of the plasma characteristics was attempted, and the dependence of the plasma parameters on the operating condition was studied.

II. EXPERIMENTAL SETUP

Figure 1 shows a schematic view of the atmospheric MIP system under study. It consists of a 2.45 GHz microwave generator, WR-284 wave guide components, and a field applicator. To maintain the reflected power below 1% of the forward power, a three stub tuner was used. The reflected power was dumped into a water load through the circulator. The forward and reflected power were monitored by a directional coupler and a Schottky power detector. The WR-284 wave guide was tapered off to 80 mm$\times$10 mm to increase the electric field strength in the region of interest. A fused silica tube of 18 mm inner diameter was inserted vertically, perpendicularly to the wide wall of the wave guide, and served as the discharge tube. The distance from the wave guide center to the open end of the tube was typically several centimeters. The discharge tube was located at a quarter λ_g (wavelength of the microwave in the wave guide) away from the shorted end of the wave guide where the electric field intensity is at its maximum. This location was confirmed by an HFSS (High Frequency Structure Simulator) code simulation[12] in which the electric field intensity around the dielectric discharge tube was calculated. The top side of the discharge tube was open to the air.

A mixed gas of argon and a small amount of hydrogen (less than 1% of argon) was introduced from underneath the discharge tube to ensure a stable plasma generation, as shown in Fig. 1. The hydrogen was added to obtain a detectable level of H_β emission intensity for electron density measurement. All the measurements were performed under the same experimental conditions except that the gas flow rate and microwave power were varied.

Using a convex lens of 6.3 cm focal length, the plasma was imaged onto a screen with a 1:1 image size, and an optical fiber attached to the screen transported the local plasma emission to a spectrometer. The spectrometer used for the experiment was Chromex 250is with a 1200 grooves/mm grating. The entrance slit width was maintained at 50 μm, and the integration time of the charged coupled device (CCD) detector was set at (30–300) ms.

III. RESULTS AND DISCUSSIONS

At a relatively low microwave power level ($<$500 W) and gas flow rate [$<$2.5 liter per minute (ℓpm)], plasma filaments were observed as is often seen in other microwave plasma experiments.[13–15] As the gas flow rate was raised above (2.5–3.0) ℓpm at a fixed microwave power ($>$500 W), the plasma filaments became longer and converged to a single point that was located above the open end of the discharge tube. The distance from the end of the discharge tube to the converging point, which is denoted as H in Fig. 2, was (5–30) mm depending on the gas flow rate. With increasing the microwave power at a fixed argon flow rate, the number of the plasma filaments increased and each filament became longer within the discharge tube toward the gas injection entrance, i.e., toward the bottom side of the discharge tube. However, H was almost unchanged with the microwave power level.

In the range of (650–950) W and above 3.0 ℓpm, a plasma flame was formed starting from the converging point, as shown in Fig. 2(a). The length L from the converging point and the diameter D at the half-length of the plasma flame region were measured as a function of microwave power. As shown in Fig. 2(b) where the gas flow rate was 4 ℓpm, L and D were (40–90) mm and (12–20) mm, respectively, and they increased almost linearly as microwave power P was increased. Supposing that the shape of the plasma flame is roughly two identical cones stacked one on top of the other, the plasma volume is proportional to P^3. In the range of (3.0–5.0) ℓpm, the plasma volume had little dependence on flow rate.

Above the critical gas flow rate (5.0 ℓpm in the case of 950 W), however, the vertical position of the converging point was further raised, i.e., H was increased due to the

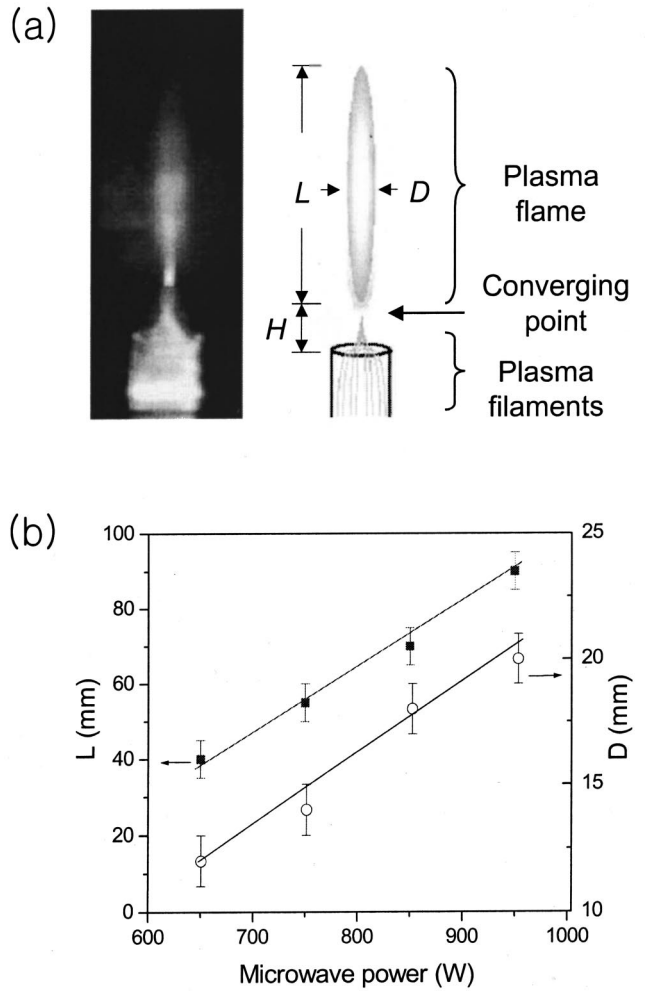

FIG. 2. (a) Three distinctive plasma regions. H, L, and D are functions of microwave power and gas flow rate. (b) The length L and the diameter D of the plasma flame region as functions of microwave power at 4 ℓpm.

extended filaments. At the same time, both L and D were decreased as the flow rate was increased. At about 10 ℓpm, the plasma flame completely disappeared, leaving only filaments. With these operation boundaries established, experiments were mostly performed at (650–950) W and (3.0–5.0) ℓpm.

A. Filament-converging point

Due to its high emission intensity, the argon atom excitation temperature, rotational temperature, and electron density were measured at the filament-converging point by OES. Each of the diagnostic methods is briefly described as follows.

The excitation temperature of Ar I lines was measured by using the Boltzmann plot method. The atomic emission intensity (I_{pq}) of the transition from level p to level q depends on the transition probability (A_{pq}) and absolute population of the atomic level (n_p), as shown in the following equation:

$$I_{pq}=n_p A_{pq} h\nu, \tag{3.1}$$

where h is the Planck constant and ν is the photon frequency

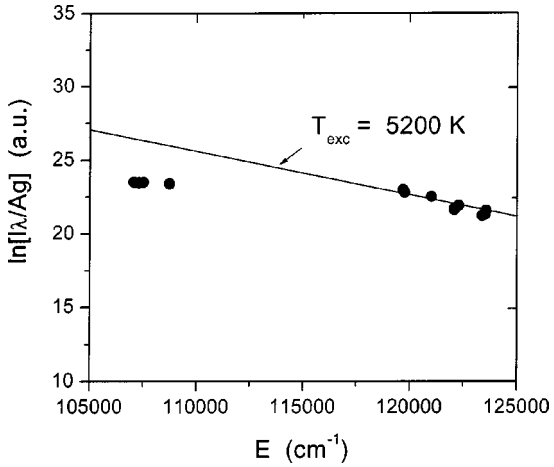

FIG. 3. Boltzmann plot of Ar I levels yielding the excitation temperature at the filament-converging point. Because of the underpopulated low energy state relative to the Saha equilibrium state, it is believed that the plasma is of the recombining type. 850 W and 4.0 ℓpm.

corresponding to the $p\rightarrow q$ transition. Assuming a Boltzmann distribution of the population of the atomic level, the emission intensity is expressed[16,17] as

$$I_{pq}=\frac{hc}{\lambda}\frac{ng_pA_{pq}}{Z(T_{\mathrm{exc}})}\exp\left(-\frac{E_p}{k_BT_{\mathrm{exc}}}\right), \tag{3.2}$$

$$\ln\left(\frac{I_{pq}\lambda}{A_{pq}g_p}\right)=-1.4388\times\frac{E_p}{T_{\mathrm{exc}}}+\text{constant}, \tag{3.3}$$

where n is the number density of bound electrons in all ionization states, $Z(T_{\mathrm{exc}})$ is the partition function, c is the speed of light in vacuum, λ is the wavelength of the corresponding transition, g_p is the statistical weight of level p and E_p is its energy in cm^{-1}, k_B is the Boltzmann constant, and T_{exc} is the excitation temperature in Kelvin. From the measurement of intensity and wavelength, a Boltzmann plot is obtained.

Figure 3 shows the Boltzmann plot of the experimental data obtained at 850 W and 4.0 ℓpm. The excitation temperature found by linear fitting of the high energy level data is about 5200 K. As shown in the figure, the low energy state is underpopulated relative to the Saha equilibrium state, showing recombining plasma characteristics.[18]

As this atmospheric plasma is produced in open air, OH molecular lines ($A\,^2\Sigma^+, \nu=0\rightarrow X\,^2\Pi, \nu'=0$, 306–310 nm) are observed in the emission spectrum due to water molecules in the air. Assuming the rotational temperature T_{rot} of OH molecules to be equal to the gas temperature of the plasma,[19,20] the gas temperature can be determined from T_{rot} using the Boltzmann plot method.[17,19,20] However, T_{rot} was determined in this work by comparing the synthetic OH spectrum with the measured spectrum obtained at a relatively low spectral resolution.[21,22] The theoretical OH spectrum intensity is given[17,19] by

$$I=D_0\,k^4 S\exp\left(-\frac{E_r}{k_BT_{\mathrm{rot}}}\right), \tag{3.4}$$

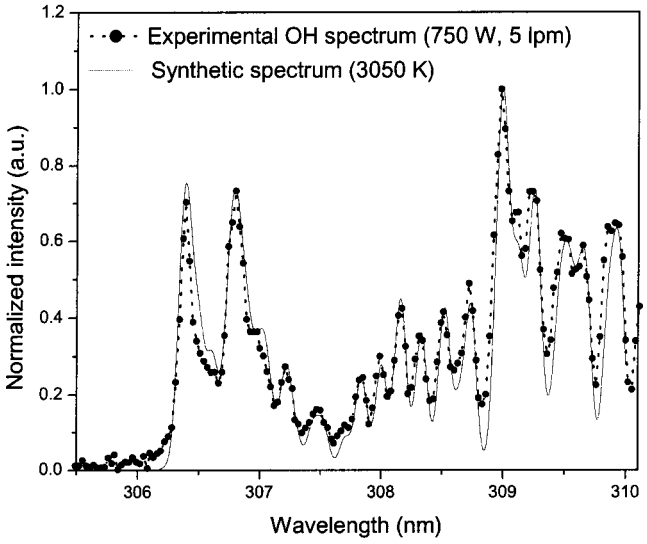

FIG. 4. Comparison of the experimental data with the synthetic OH spectrum yielding a rotational temperature of 3050 K at the filament-converging point. 750 W, 5.0 ℓpm.

where k is the wave number, S is the oscillator strength, and D_0 is a coefficient containing the rotational partition function, and E_r is the rotational energy level. D_0 and E_r are expressed as

$$D_0 = \frac{C(J'+J''+1)}{Q_r}, \tag{3.5}$$

$$E_r = B_v hcJ'(J'+1), \tag{3.6}$$

where C is a constant depending on the change of dipole moment and total number of molecules in the initial vibrational state, Q_r is the rotational partition function, J' and J'' are the upper and lower state, respectively, and B_v is a rotational constant in the state of the vibrational quantum number v.

Figure 4 depicts the comparison of the experimental data (750 W, 5.0 ℓpm) with the synthetic OH spectrum at 3050 K, and the two are shown to be in good agreement. The synthetic spectrum was obtained from Eq. (3.4) based on the data of Dieke and Crosswhite.[19]

The electron density was measured by the Stark broadening width of the hydrogen H_β line that is emitted from the plasma. Based on Stark broadening theory,[23,24] the electron density n_e in a high pressure plasma is expressed[25] as

$$n_e = 8.02\times 10^{12}\left(\frac{\Delta\lambda_{1/2}}{\alpha_{1/2}}\right)^{3/2}, \tag{3.7}$$

where $\Delta\lambda_{1/2}$ (Å) is the full-width at half-maximum (FWHM) of the hydrogen line, and $\alpha_{1/2}$ is the reduced wavelength (Å/cgs field strength) that is tabulated in Ref. 23. To obtain the Stark broadening width of the hydrogen line, Doppler broadening and instrumental broadening effects must be excluded.

The obtained H_β line profile was fitted with the Voigt function[16,17,23,25] such as the one shown in Fig 5. Through the deconvolution process, it was obtained that the Gaussian instrumental broadening width was 1.1 Å and the Lorentzian

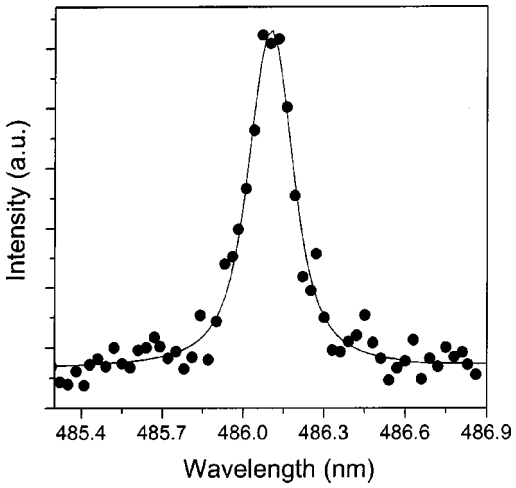

FIG. 5. Voigt function fitting of the experimental H_β spectral line for obtaining electron density at the filament-converging point. 850 W, 3.0 ℓpm.

Stark broadening width was (1.2–1.6) Å. The instrumental broadening was independently checked using a He–Ne laser and a mercury lamp. The Doppler broadening due to the thermal motion of particles was negligible relative to the instrumental and Stark broadening because the Doppler broadening width of 3000 K hydrogen neutral atoms is only about 0.18 Å. When microwave power and gas flow rate were set at 850 W and 3.0 ℓpm, respectively, the measured electron density was about 5.3×10^{14} cm^{-3}.

With the diagnostic methods described above, $T_{\rm exc}$, $T_{\rm rot}$, and n_e were measured as the gas flow rate and microwave power level were varied in the ranges of (3.0–5.0) ℓpm and (650–950) W.

Figure 6 shows the measured excitation temperature where $T_{\rm exc}$ is about (5000–5800) K. There is no significant dependence of $T_{\rm exc}$ on gas flow rate and microwave power as could be expected, i.e., the electron temperature does not depend much on these parameters.

The measured rotational temperature is about (2800–3400) K as shown in Fig. 7. In contrast to $T_{\rm exc}$, $T_{\rm rot}$ increases with the increase in microwave power. This is because more

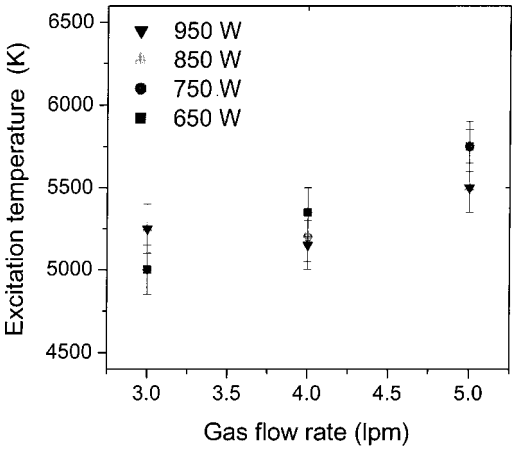

FIG. 6. Excitation temperature as a function of argon flow rate at various microwave power levels, as measured at the filament-converging point.

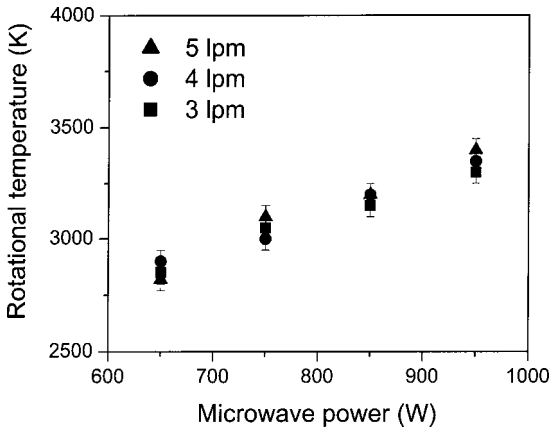

FIG. 7. Rotational temperature as a function of microwave power at various gas flow rates, at the filament-converging point.

energetic electrons collide elastically with heavy neutral particles. On the other hand, as the gas flow rate increases, T_{rot} shows little change. Although an increase in the gas flow rate is usually expected to cool down a discharge, the effect of the increment from 3.0 to 5.0 ℓpm does not seem to be significant for cooling it, most probably because of the filamentary structure of the argon discharge.

Figure 8 shows the electron density obtained from the H_β line broadening width where n_e is about $(5.0-8.0)\times 10^{14}\ \mathrm{cm}^{-3}$. It depends on the gas flow rate, but not on microwave power. This dependence was also observed in the measured H_α linewidth.

As mentioned above, the increase of microwave power brought about an expansion of the plasma flame [Fig. 2(b)] and increase of the gas temperature (Fig. 7) with little change in the electron density. However, the electron density increases as the gas flow rate increases. This finding of a dependence of electron density on gas flow rate and microwave power is different from findings in other atmospheric microwave plasma experiments.[26–28] This may be attributed to different discharge conditions in that the gas fluid element speed is significantly different due to a smaller gas flow rate and larger discharge tube diameter. The microwave power is concentrated on the active zone called the surface-wave launching place in the surfaguide.[29,30] The electric field in the active zone is very strong due to the microwave power concentration. A simulation study of electromagnetic fields, whose profile is very similar to the previous study,[30] indicates that the electric field intensity at the surface-wave launching place is about 8 kV/cm for 1 kW microwave power.[31] Recall that the electron temperature in the plasma is almost linearly proportional to the electric field intensity.[32] The higher the electron temperature is the more efficiently the ionization of neutrals, abundantly generating electrons. Therefore, most of the microwave power is absorbed into the gas fluid element in this active zone by ohmic heating, thereby effectively ionizing neutrals in this place.

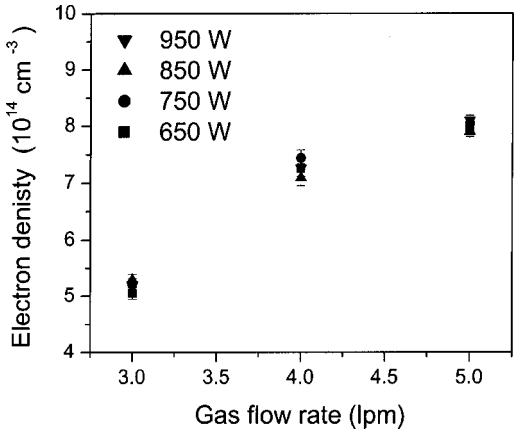

FIG. 8. Electron density as a function of argon flow rate at various microwave power levels, at the filament-converging point.

Assuming that the electron density at the ionizing zone is n_{e0}, the electron density may decrease as the gas fluid element drifts out from the zone. The rate equation of the electron density can then be expressed as

$$\frac{dn_e(z)}{dz} = -\frac{\alpha_r}{v} n_e^2, \tag{3.8}$$

where the radiative recombination coefficient of the argon plasma α_r is of the order of 10^{-13} cm^3/s for 1 eV electron temperature, and z and v are the drift distance and speed, respectively, of the fluid element. When an ion and electron collide, they have a finite probability of recombining into a neutral atom. To conserve momentum, a third body must be present. In the case of radiative recombination where the third body is an emitted photon, the plasma rate equation becomes[33]

$$\frac{dn_e(z)}{dt} = -\alpha_r n_e^2. \tag{3.9}$$

Assuming a uniform speed of the gas fluid element, and integrating Eq. (3.8) with respect to z, the electron density $n_e(z)$ at the propagation distance z from the ionizing zone is given by[34]

$$\frac{n_e(z)}{n_{e0}} = \frac{1}{1+\alpha_r n_{e0} z/v}, \tag{3.10}$$

which determines the ion density decay in terms of the propagation distance z. The axial speed of the fluid element v in cm/s is calculated[34] to be

$$v = 16\frac{\xi T_{\mathrm{gas}}}{S T_r}, \tag{3.11}$$

where ξ is the gas flow rate in ℓpm, S is the plasma cross-sectional area in cm^2, T_{gas} is the gas temperature, and T_r is the room temperature in Kelvin. If $\alpha_r n_{e0} z/v \ll 1$, then $n_e(z)/n_{e0} \simeq (1-\alpha_r n_{e0} z/v)$, i.e., the electron density decreases linearly with respect to z. This type of axial density profile is seen in other surface-wave sustained discharges.[26,29,35]

Since $\alpha_r n_{e0} z/v \gg 1$ in our experimental case, Eq. (3.10) is simplified to

$$n_e \simeq \frac{1}{\alpha_r z/v}, \tag{3.12}$$

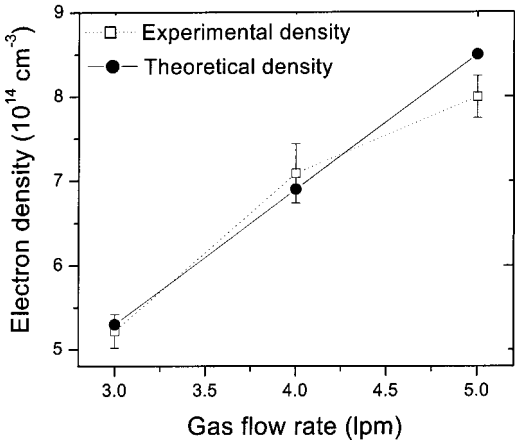

FIG. 9. Comparison of the theoretically and experimentally obtained electron density as a function of gas flow rate.

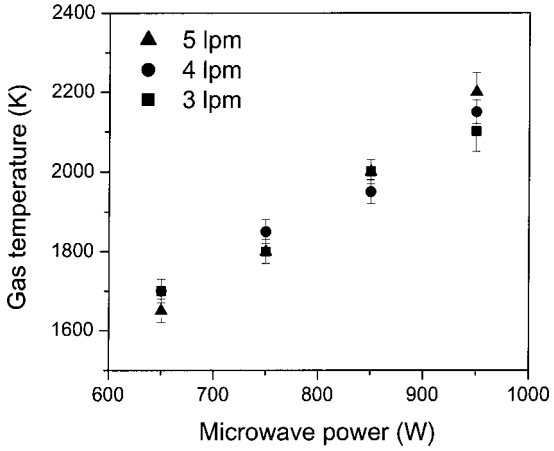

FIG. 10. Gas temperature at 1 cm above the converging point obtained from OH molecular emission lines.

which is independent of the initial electron density n_{e0}. Inserting Eq. (3.11) into Eq. (3.12), the electron density at z is finally given by

$$n_e = \frac{16 T_{\mathrm{gas}}}{\alpha_r z S T_r} \xi. \tag{3.13}$$

This indicates that $n_e(z)$ is linearly proportional to the gas flow rate ξ. Figure 9 shows the theoretical electron density obtained by Eq. (3.13) where least square fitting of the measured data was performed by changing α_r.

In summary, it was observed that the volume of the plasma flame [Fig. 2(b)] and the gas temperature (Fig. 7) were increased at higher microwave power levels. On the other hand, higher gas flow rates increased the electron density (Fig. 8).

B. Plasma flame

At the filament-converging point, the emission intensity of the H_α spectral line was typically (10–20) times higher than that of the H_β line. Because of low emission intensity, it was not possible to observe the H_β line at all in the region above the converging point. Although the H_α line was barely measurable at 1 cm above the converging point, we were able to observe that the Stark broadening width was much smaller than that at the converging point which means very small electron density above the converging point. Therefore, the converging point is believed to be the end of the surface-wave sustained plasma, and the region above that point is the plasma flame in which the disappearance of the free electron population is due to the dominant electron–ion collisional radiative recombination.

Due to the relatively low emission intensity, only rotational temperature was measured by the spectroscopic method at 1 cm above the filament-converging point. As shown in Fig. 10, the gas temperature was about (1650–2200) K, which was lower than the value (2800–3400 K) at the converging point. Similar to the converging point case, it was linearly proportional to the microwave power.

At other vertical positions in the plasma flame, the gas temperature was measured by using a calibrated thermocouple [Fig. 11(a)]. Since the length of the plasma flame increased with the microwave power as shown in Fig. 2(b), the location of the same gas temperature shifted away from the converging point as the microwave power increased. Figure 11(b) is the plot showing the axial profile of the gas

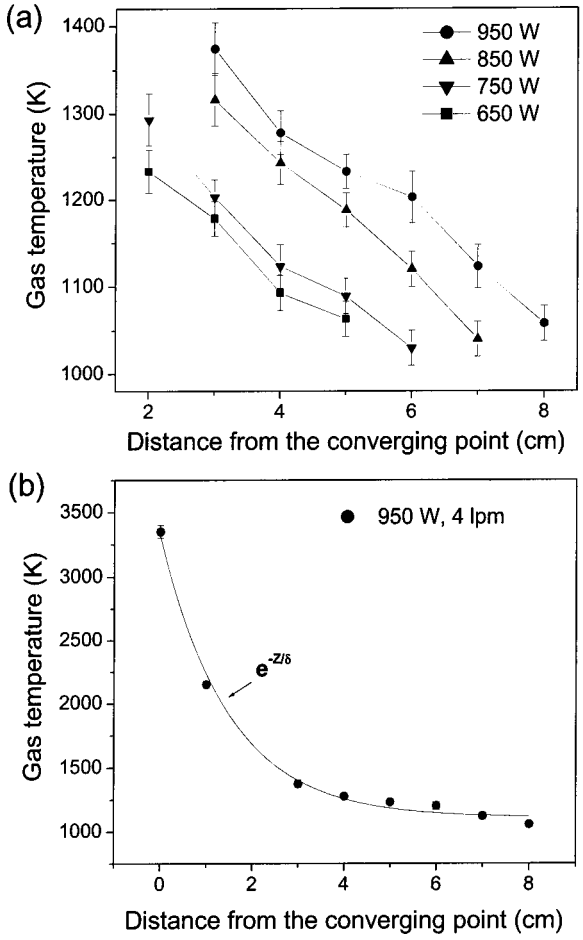

FIG. 11. (a) Vertical profile of the gas temperature in the plasma flame measured by a thermocouple. (b) Exponential decrease of the gas temperature from the converging point to the tail of the plasma flame. 950 W and 4 ℓpm.

temperature from the converging point through the plasma flame at 950 W and 4 ℓpm, where an exponential decrease was seen. The e-folding length δ was 0.9 cm to 1.5 cm as the microwave power increased from 650 W to 950 W. In the plasma flame, the gas temperature showed little dependence on gas flow rate.

IV. SUMMARY

Plasma was produced in a simple open-ended dielectric discharge tube at atmospheric pressure using a 2.45 GHz microwave system. Three distinctive plasma regions were observed with the assistance of argon gas flow: plasma filaments exiting from the discharge tube, converging point of these filaments, and a plasma flame. The existence of the three regions is similarly found in other atmospheric plasma sources such as TIA[4] and MPT.[6]

At the filament-converging point, OES was performed to measure excitation temperature, rotational temperature, and electron density. The excitation temperature was obtained from the Boltzmann plot of emitted Ar I lines, and the rotational temperature was measured by comparing with synthetic OH molecular spectrum. The electron density was obtained through deconvolution of Voigt function fitting of the H_β spectral line. In the operating ranges of (650–950) W and (3.0–5.0) ℓpm, it was found that $5000\ \mathrm{K} < T_{\mathrm{exc}} < 5800\ \mathrm{K}$, $2800\ \mathrm{K} < T_{\mathrm{rot}} < 3400\ \mathrm{K}$, and $5.0\times10^{14}\ \mathrm{cm}^{-3} < n_e < 8.0\times10^{14}\ \mathrm{cm}^{-3}$.

It was observed that the gas temperature at the filament-converging point increased along with microwave power. Therefore, in the operating range where most of the measurements were performed, some of the microwave power was consumed in heating up the neutral particles leading to the expansion of the plasma flame. On the other hand, higher gas flow rates increased the electron density with little change in gas temperature.

In the plasma flame, rotational temperature was measured by OES at only 1 cm above the filament-converging point due to the relatively low emission intensity. At other vertical positions, the gas temperature was measured using a thermocouple. At 850 W and 4 ℓpm, the gas temperature was about 3200 K at the converging point, 1950 K at 1 cm above the converging point, and then decreased from 1300 K to 1050 K in 3 cm to 7 cm from the converging point, which showed exponential decrease. In the plasma flame, the gas temperature showed little dependence on gas flow rate.

ACKNOWLEDGMENTS

This work was supported by Grant No. R01-2000-00254 from the Korea Science and Engineering Foundation, and the BK21 Project.

[1] J. R. Roth, *Industrial Plasma Engineering Vol. 1: Principles* (IOP, Bristol, 1995).
[2] P. P. Woskov, D. Y. Rhee, P. Thoma, D. R. Cohn, J. E. Surma, and C. H. Titus, Rev. Sci. Instrum. **67**, 3700 (1996).
[3] M. Moisan, J. Hubert, J. Margot, G. Sauvé, and Z. Zakrzewski, *Microwave Discharge: Fundamentals and Applications*, edited by C. M. Ferreira and M. Moisan (Plenum, New York, 1992), Chap. 1.
[4] J. Jonkers, J. M. de Regt, J. A. M. van der Mullen, H. O. C. Vos, F. P. J. de Groote, and E. H. A. Timmermans, Spectrochim. Acta, Part B **51**, 1385 (1996).
[5] M. Moisan, G. Sauvé, Z. Zakrzewski, and J. Hubert, Plasma Sources Sci. Technol. **3**, 584 (1994).
[6] C. Prokisch, A. M. Bilgic, E. Voges, J. A. C. Broekaert, J. Jonkers, M. van Sande, and J. A. M. van der Mullen, Spectrochim. Acta, Part B **54**, 1253 (1990).
[7] Y. Okamoto, Plasma Sources Sci. Technol. **5**, 648 (1996).
[8] C. I. M. Beenakker, Spectrochim. Acta, Part B **31**, 483 (1976).
[9] E. A. H. Timmermans, Ph.D. thesis, Eidenhoven University Technology, 1999.
[10] H. S. Uhm, Phys. Plasmas **6**, 4366 (1999).
[11] K. M. Green, M. C. Borras, P. P. Woskov, G. J. Flores III, K. Hadidi, and P. Thomas, IEEE Trans. Plasma Sci. **29**, 399 (2001).
[12] HFSS Release 8.0 Ansoft; Four Station Square, Suite 200, Pittsburgh, PA 15219-1119.
[13] Y. Kabouzi, M. D. Calzada, M. Moisan, K. C. Tran, and C. Trassy, J. Appl. Phys. **91**, 1008 (2002).
[14] N. Djermanova, D. Grozev, K. Kirov, K. Makasheva, A. Shivarova, and Ts. Tsvetkov, J. Appl. Phys. **86**, 738 (1999).
[15] V. B. Gil'denberg and A. V. Kim, Sov. J. Plasma Phys. **6**, 496 (1980).
[16] W. Lochte-Holtgreven, *Plasma Diagnostics* (North-Holland, Amsterdam, 1968), Chap. 1, 3.
[17] P. W. J. M. Boumans, *Inductively Coupled Plasma Emission Spectroscopy Part 2* (Wiley, New York, 1987), Chap. 10.
[18] J. A. M. van der Mullen, Phys. Rep. **191**, 109 (1990).
[19] G. H. Dieke and H. M. Crosswhite, J. Quant. Spectrosc. Radiat. Transf. **2**, 97 (1962).
[20] G. Herzberg, *Molecular Spectra and Molecular Structure: 1. Spectra of Diatomic Molecules*, 2nd ed. (Van Nostrand, Princeton, 1964).
[21] S. Pellerin, J. M. Cormier, F. Richard, K. Musiol, and J. Chapelle, J. Phys. D **29**, 726 (1996).
[22] C. de Izarra, J. Phys. D **33**, 1697 (2000).
[23] H. R. Griem, *Spectral Line Broadening by Plasma* (Academic, New York, 1974).
[24] H. R. Griem, *Principles of Plasma Spectroscopy* (Cambridge University Press, Cambridge, MA, 1997).
[25] J. Ashkenazy, R. Kipper, and M. Caner, Phys. Rev. A **43**, 5568 (1991).
[26] M. C. Garcia, A. Rodero, A. Sola, and A. Gamero, Spectrochim. Acta, Part B **55**, 1733 (1996).
[27] A. Rodero, M. C. Garcia, M. C. Quintero, A. Sola, and A. Gamero, J. Phys. D **29**, 681 (1996).
[28] P. G. Brown, T. J. Brotherton, J. M. Workman, and J. A. Caruso, Appl. Spectrosc. **41**, 774 (1987).
[29] M. Moisan and Z. Zakrzewski, J. Phys. D **24**, 1025 (1991).
[30] M. Moisan, Z. Zakrzewski, R. Etemadi, and J. C. Rostaing, J. Appl. Phys. **83**, 5691 (1998).
[31] Y. C. Hong (private communications).
[32] H. S. Uhm, E. H. Choi, and G. Cho, Phys. Plasmas **7**, 2744 (2000).
[33] F. F. Chen, *Introduction to Plasma Physics and Controlled Fusion* (Plenum, New York, 1984), Chap. 5.
[34] H. S. Uhm and S. H. Hong, Combust. Sci. Technol. **152**, 147 (2000).
[35] K. Kirov, K. Makasheva, and A. Shivarova, Vacuum **58**, 280 (2000).